

Forschungszentrum Karlsruhe

Technik und Umwelt

Wissenschaftliche Berichte

FZKA 6448

FE-Analysis of a Current Lead

A. Grünhagen

Institut für Medizintechnik und Biophysik

Projekt Kernfusion

Forschungszentrum Karlsruhe GmbH, Karlsruhe

2000

FE-Analyse einer Stromzuführung

Zusammenfassung:

Die 80 kA Stromzuführung und der Bus Bar Type 2, eingesetzt im Spulentest TFMC in TOSKA, werden über Klammern verbunden. Sie dienen zur Erhöhung der Flächenpressung im Kontaktbereich und führen somit zu einer Reduktion des Kontaktwiderstandes. Außerdem verringert sich infolge des reduzierten Kontaktwiderstandes die aufzuwendende Kälteleistung. Die Festigkeitsberechnungen mit dem Finite-Element-Programm ABAQUS zeigen ein unkritisches Verhalten der Stromzuführung.

FE-Analysis of a current lead

Abstract:

The 80 kA current lead and the bus bar type 2 required in the coil test TFMC in TOSKA are joined with clamps. They increase the surface pressure in the area of contact and decrease thus the resistance of contact. Moreover, lower resistance of contact decrease the required refrigerating capacity. The strength calculations with the finite element program ABAQUS show an uncritical behavior of the current lead.

Contents

1. Introduction	1
2. Finite Element Analysis	2
2.1 Objective	2
2.2 Model Description	5
2.3 Results	9
3. Conclusion	20
4. References	21

1. Introduction

The additional clamp was designed by ITP in order to increase the pressure acting in the contact surface area from 5 to 20 MPa. This measure leads to a reduction of the resistance of contact as well as of the required refrigerating capacity. The EU joint concept used in the SS FSJS (**S**tainless **S**teel **F**ull **S**ize **J**oint **S**ample) and the TFMC (**T**oroidal **F**ield **M**odel **C**oil) is based on the use of copper/steel explosion bonded plates for the joint box manufacture. The cable is compacted with $2.0 \cdot 10^6$ N inside the box against the copper sole up to a 25% final void fraction. The joint box is then tightly TIG (**T**ungsten **I**ncert**G**as) welded before the reaction heat treatment. The electrical contact between cable and copper sole is then ensured by the residual compaction force after cooldown at 4K and by the compaction force of the clamps.

2. Finite Element Analysis

2.1 Objective

The clamp joint shown in a general view (figure 1) and in a sectional view (figure 2) consists of 16 identical units. Each unit is built with the cable, the stamp, the steel and copper box and the lower and upper clamp. The configuration of a half unit is illustrated in a side view (figure 3).

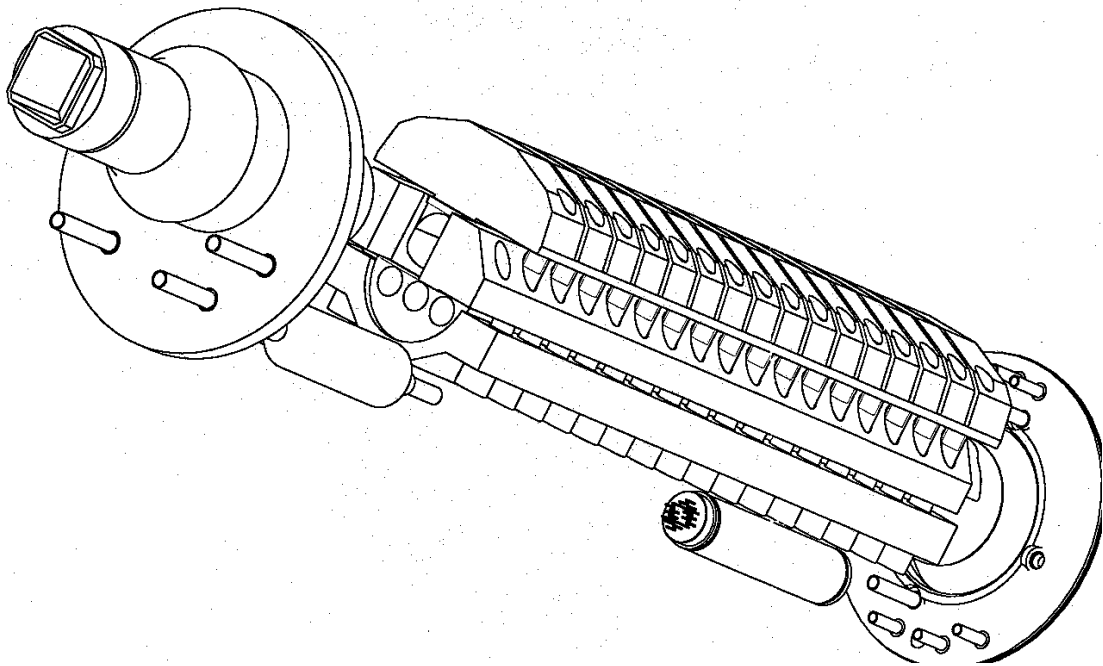


Figure 1 - Clamp joint in a general view

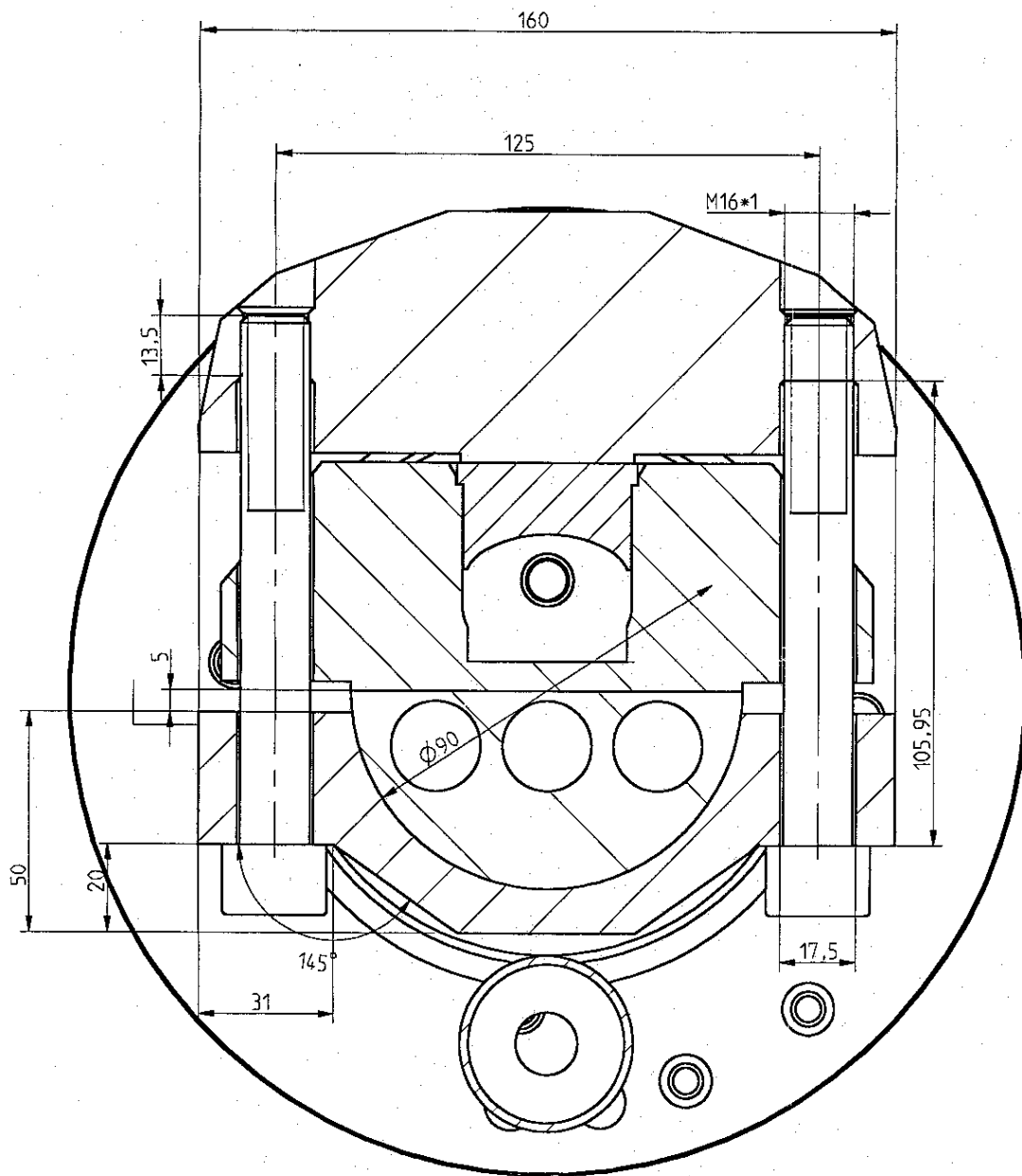
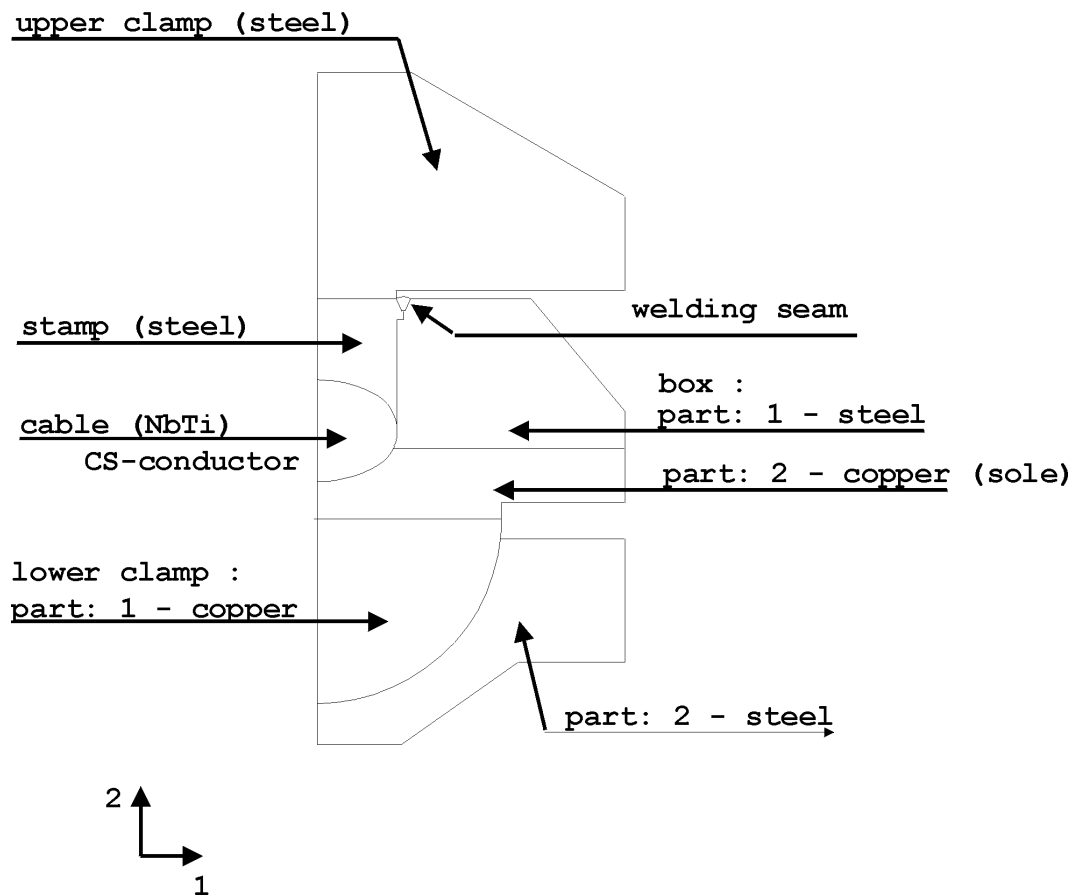


Figure 2 - Clamp joint in a sectional view



**Figure 3 - The assembly of the clamp joint
in a side view - model: A**

The cable is pressed by the stamp with $2.0 \cdot 10^6$ N against the copper sole of the box. Then the box (part : 1 - steel) is closed with the stamp by welding. The welding seam (figure 3) has a depth of $t_y=3$ mm. It is accepted that the remaining reaction force of the cable against the cover (upper clamp) amounts to $F_{C+}=+3.4 \cdot 10^5$ N. The box with the stamp and cable is held together by the lower and upper clamp. Both clamps are screwed so that the surface pressure between the copper sole of the box and copper part of the lower clamp (line c-c' in figure 6) has about the value of $p=20$ MPa. Moreover, the behavior of the welding seam in this assembly is of great interest.

The calculation of the deformations and the stresses are performed by the **F**inite **E**lement **M**ethod (**FEM**) with the program system ABAQUS /1/.

2.2 Model Description

As the clamp joint consists of 16 units of the same kind and each unit shows a symmetrical structure (figure 2), a half 2-dimensional model **A** (figures 3 and 4) was built of one unit with a constant thickness of **d=34 mm**.

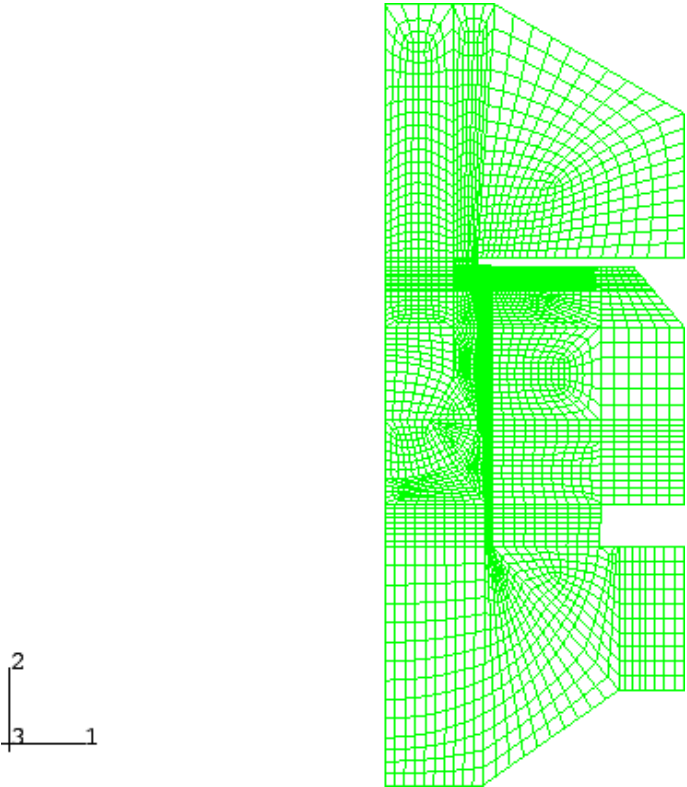
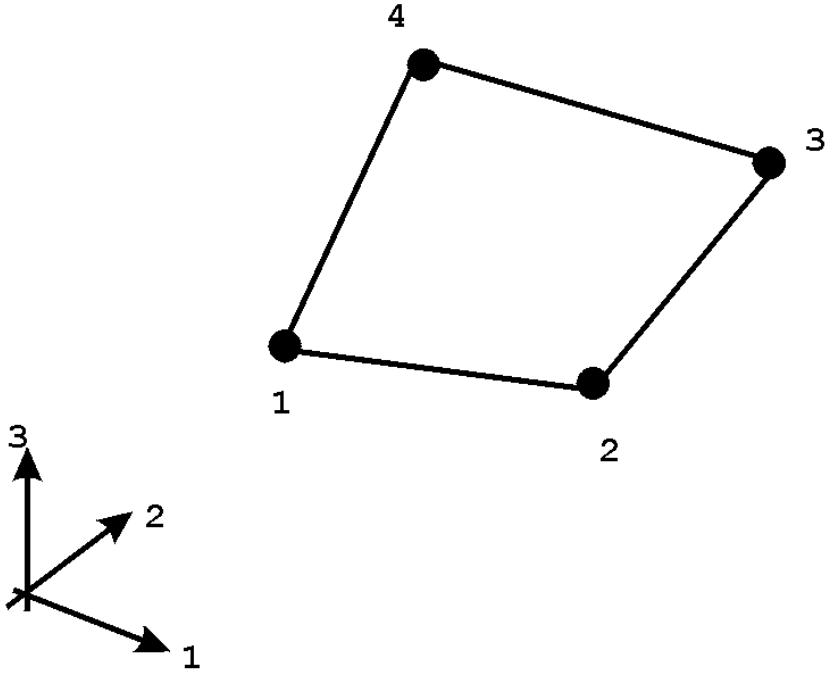


Figure 4 - FE-model: A of the clamp joint

The model was meshed with 4560 two-dimensional planar solid elements (plane strain elements - figure 5), 5021 nodes and 9708 degrees of freedom. The pre-processor ABAQUS/Pre /2/ was used for the modeling of the structure.



4-node bilinear (plane strain) element "CPE4"

Figure 5 - Choice of element

The model of the **clamp joint** is fixed in the axis of symmetry S-S' (figure 6). This means that deformations are suppressed in 1-direction and rotations round the 2- and 3-axis. Moreover, the model is supported elastically in 2-direction with a spring element.

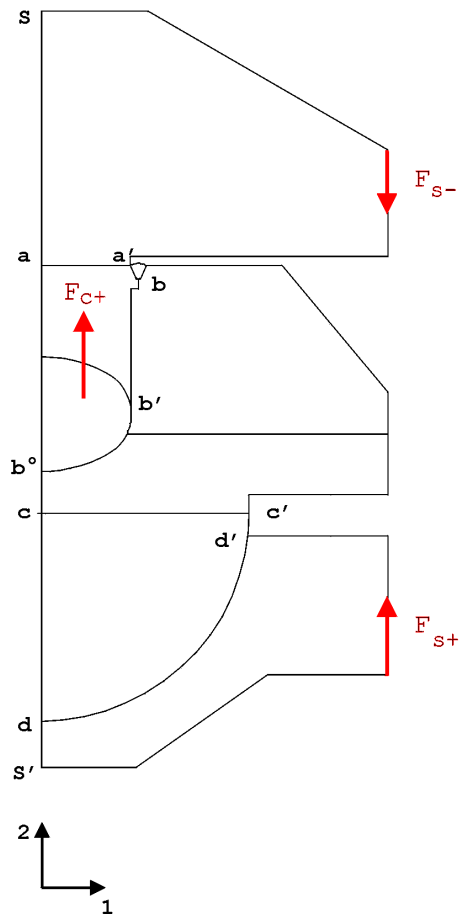


Figure 6 - Boundary conditions and presentation of the forces

The zone between upper clamp and stamp (line a-a'), between box (part:1 - steel, part:2 -copper) and stamp/cable (line b-b'-b^o), between box (part:2 -copper) and lower clamp (part:1 - copper) (line c-c') as well as between part:1 - copper and part:2 - steel of the lower clamp (line d-d') are modelled with contact elements without friction. All these zones are illustrated in figure 6.

The stamp/cable presses against the upper clamp with a total force of $F_{C+}=+3.4 \cdot 10^5$ N. Related to one unit, the force has a value of $F_{C+}/unit=+1.0414 \cdot 10^4$ N. The upper and lower clamp is screwed together with $F_{S+}=+4.0 \cdot 10^5$ N and $F_{S-}=-4.0 \cdot 10^5$ N (figure 6).

The material behavior of the **clamp joint** is assumed to be isotropic and all material data are summarized in Table 1.

	E-Modulus [MPa]	Poisson's ratio ν
upper clamp - steel (1.4571)	2.10e+05	0.3
stamp - steel (1.4571)	2.10e+05	0.3
cable - NbTi	1.10e+05	0.3
box part: 1 - steel (1.4571)	2.10e+05	0.3
box part: 2 - copper	1.25e+05	0.3
lower clamp - steel (1.4571) part: 1	2.10e+05	0.3
lower clamp - copper part: 2	1.25e+05	0.3

Table 1

2.3 Results

The linear, static calculations of the deformations and stresses were performed with the finite element program **ABAQUS** /1/. The results were plotted with the post-processor **ABAQUS/Post** /3/.

In figures 7 through 15 the distribution of the von Mises stress is illustrated in discrete filled color levels on a detail of the structure. Each colored contour corresponds to a range bounded by the values indicated on the similarly colored band within the legend. Moreover, it is difficult to show the stress distribution on the surface (figures 7 and 14) of the upper clamp and of the box because there is not such a great variety of the values.

The von Mises stress of the box shows a homogeneous distribution (average stress $\underline{\sigma}_V=150.0$ MPa) except for the area of the welding seam and of the shoulder (figure 7 - marked with 'welding seam and shoulder'). This area is illustrated in a zoomed view (figure 8). The highest value of the von Mises stress is attained here in a very small region with $\sigma_V=454.9$ MPa. It represents superelevation of the stress. According to the principle of St. Venant, the stress values taken at a sufficient distance from the peak position (1 to 2 element lengths) decrease to about $\sigma_V=225.0$ MPa. The von Mises stresses are represented along the welding seam and the shoulder (marked line W-Z-S-W' - figure 9) in figure 10. In this representation the very small stress peak (point S) is clearly recognizable.

An additional small stress peak appears at the end of the welding seam (point Z - figures 9 and 10) with a maximum stress $\sigma_V=280.0$ MPa. In the distance of 1 to 2 element lengths the von Mises stresses are just still $\sigma_V=180.0$ MPa.

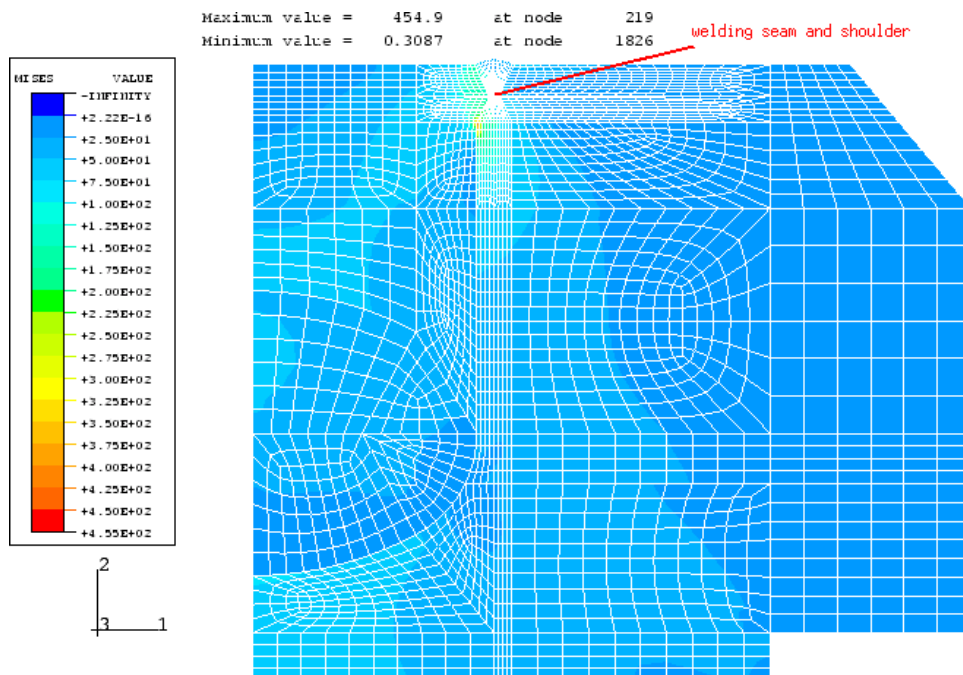


Figure 7 - Contour plot of the von Mises stresses on detail of the box

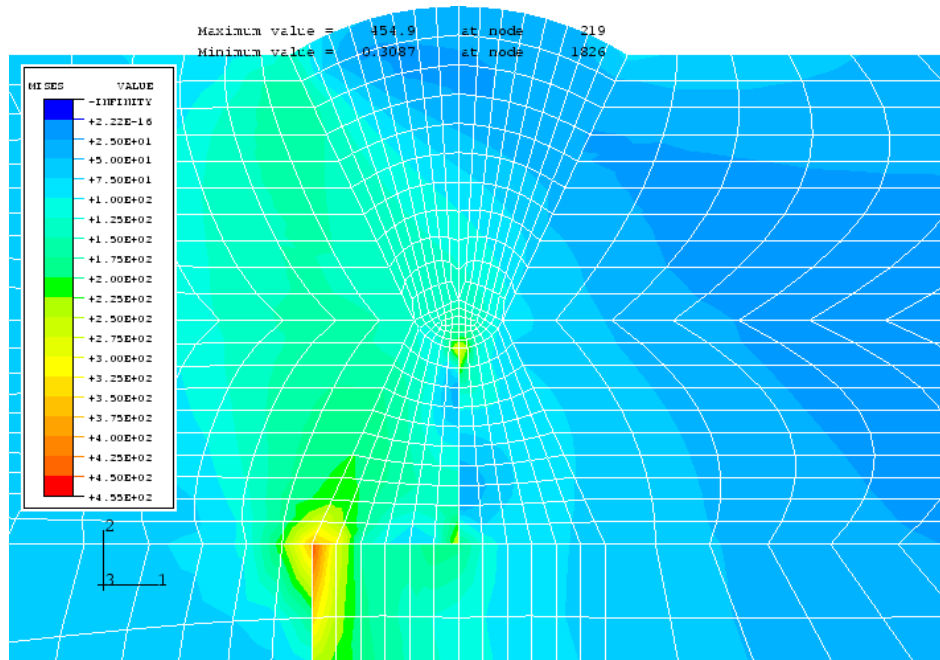


Figure 8 - Contour plot of the von Mises stresses on detail of the box - zoomed view of the marked area 'welding seam and shoulder' figure 9)

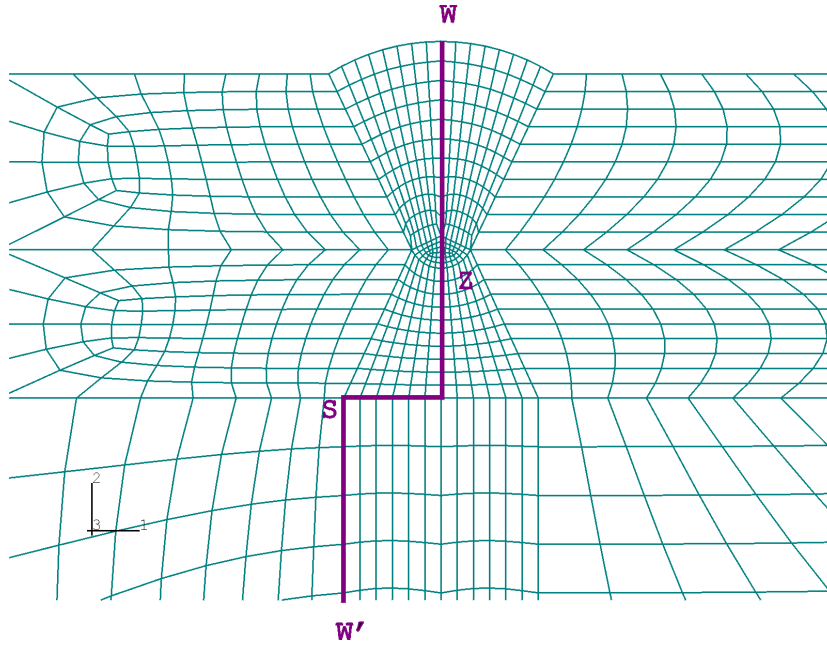


Figure 9 - Representation of the welding seam and of the shoulder

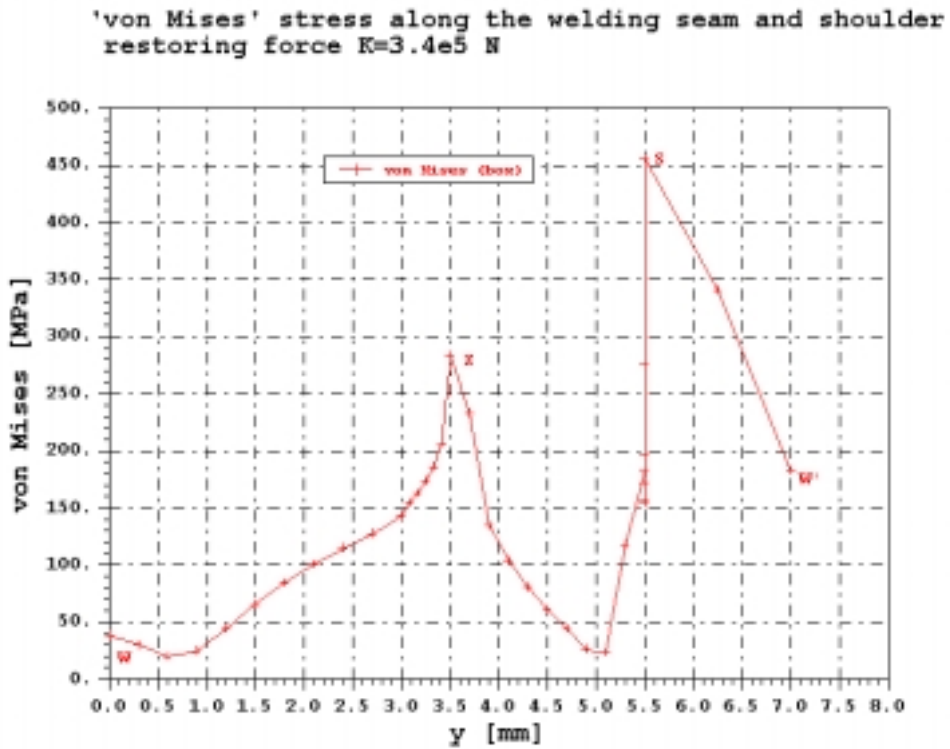
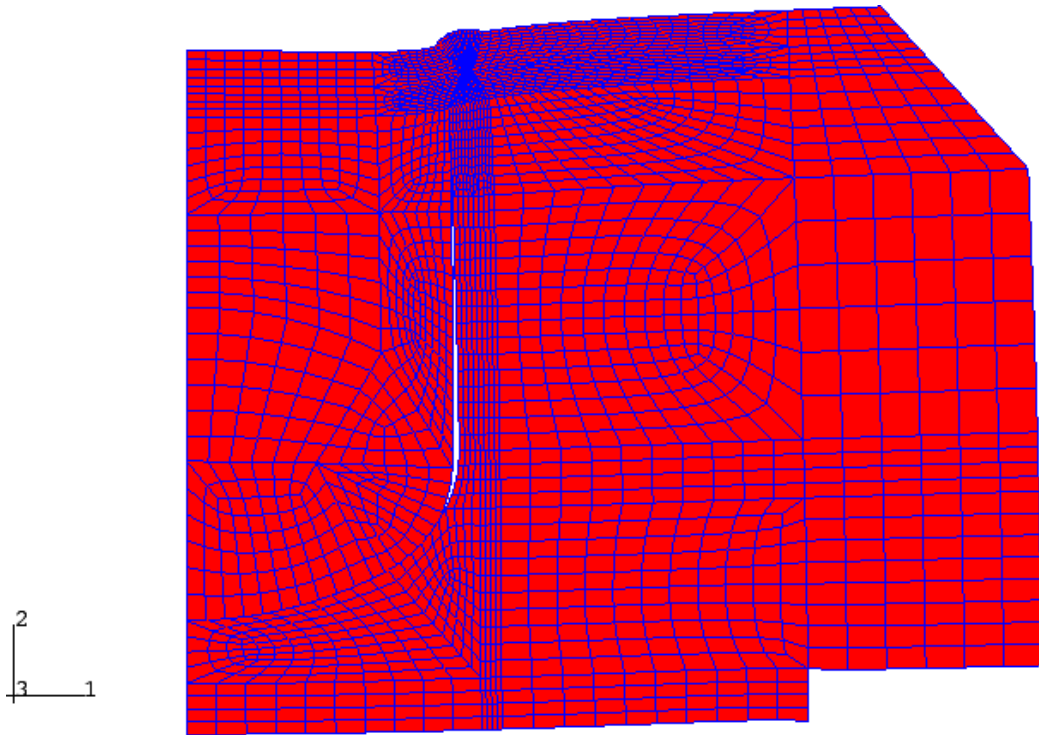


Figure 10 - von Mises stress along the welding seam and the shoulder marked line in figure 9



**Figure 11 - Front view of the deformed clamp joint
(displacement magnification factor=150)**

There is the change-over from the welding seam to the contact area between box and stamp/cable. It is difficult and too expensive to model such change-overs with finite elements in the approximation of reality. In figure 11 the deformed structure of the **clamp joint** illustrates the cause of the high stresses in the welding seam and in the shoulder. Furthermore, is shown that the stamp/cable detaches from the box (represented by the small gap in figure 11). The zone between the stamp/cable and the box (line b-b'-b^o in figure 6) was modelled with contact elements.

In the copper part of the box the highest von Mises stresses of $\sigma_v=80.98$ MPa are caused by the pressure of stamp/cable in the symmetry axis (figure 12).

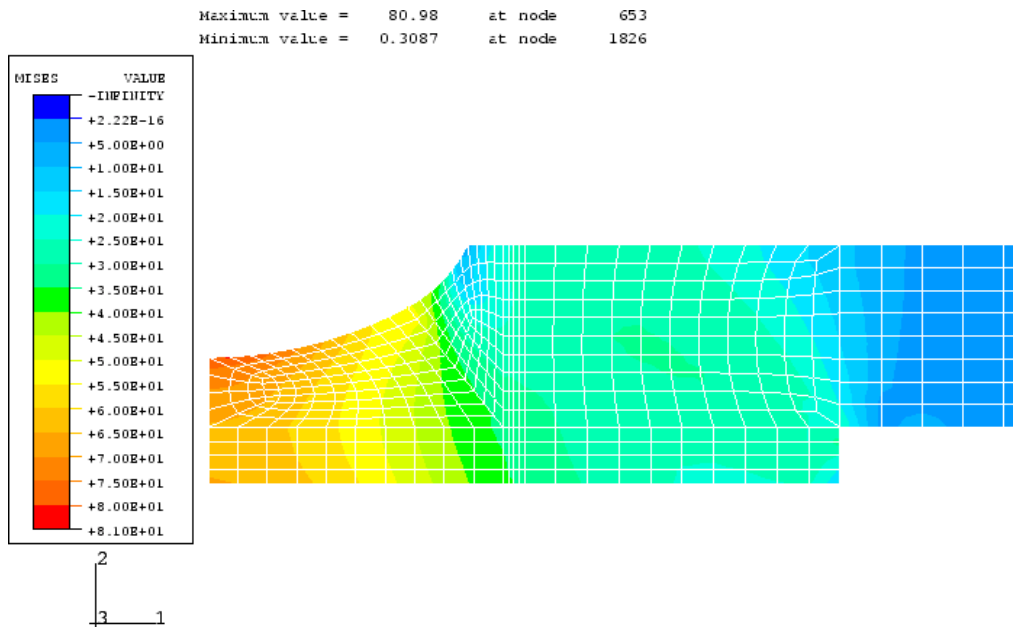


Figure 12 - Contour plot of the von Mises stresses on detail in the copper part of the box

The average stress is situated by $\underline{\sigma}_v=34.7$ MPa in this part of the clamp joint. The strength for copper has the value of $\sigma_{0.2}=100.0$ MPa.

In the contact zone to the steel part of the lower clamp two very small stress peaks (figure 13) are formed on the border of the copper part. The maximum von Mises stress amounts to $\sigma_v=111.7$ MPa. The stresses decrease at a distance of 1 to 2 element lengths to about $\sigma_v=55.0$ MPa (superelevation of stress). The average stress was calculated to $\underline{\sigma}_v=24.5$ MPa.

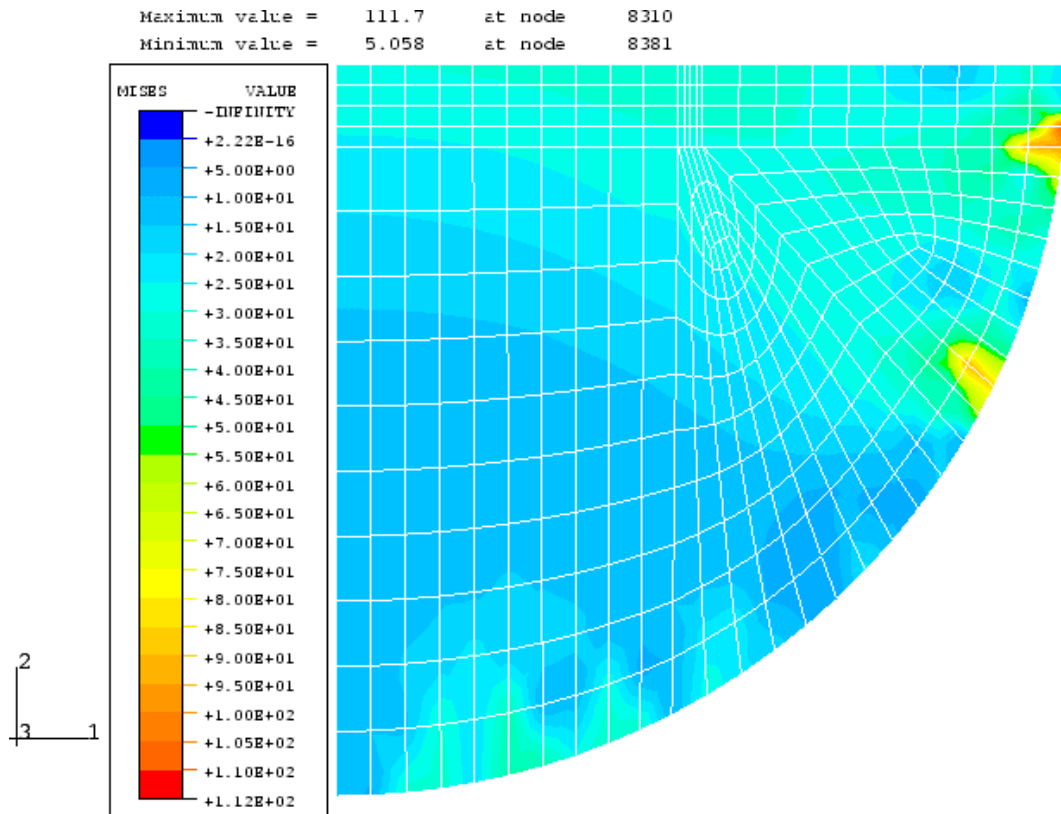


Figure 13 - Contour plot of the von Mises stresses on detail in the copper part of the lower clamp

In the upper clamp the highest von Mises stresses of $\sigma_V=487.3$ MPa are in the corner (figure 14 - marked with the letter 'E'). This area is showed in a zoomed view (figure 15). The stress peaks are caused by the bending moment of the screw connection. They represent superelevations of the stress and decrease at a distance of 1 to 2 element lengths from the peak position to about $\sigma_V=250.0$ MPa.

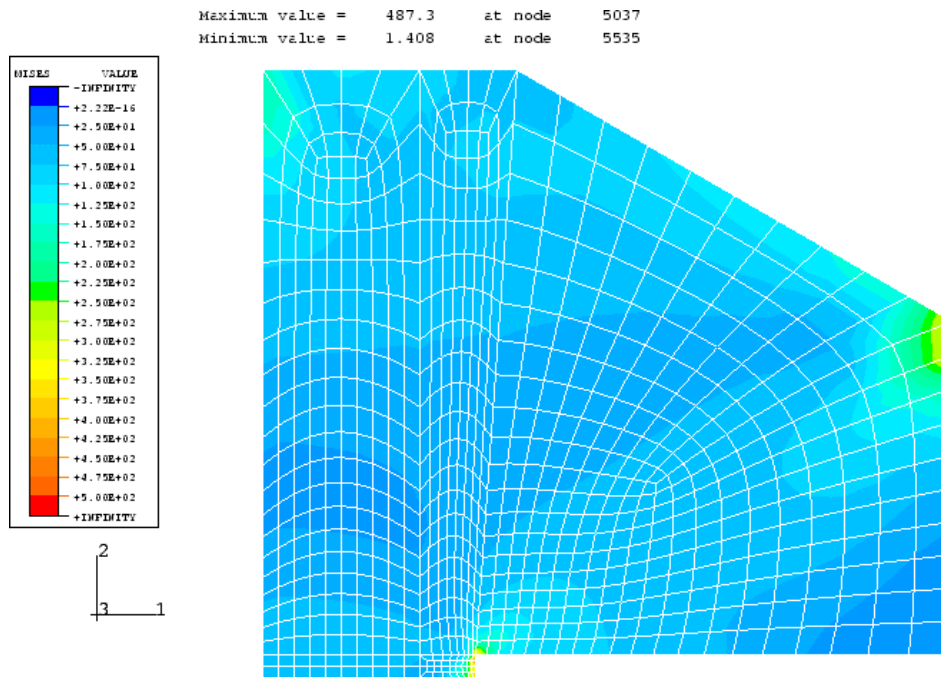


Figure 14 - Contour plot of the von Mises stresses on detail of upper clamp

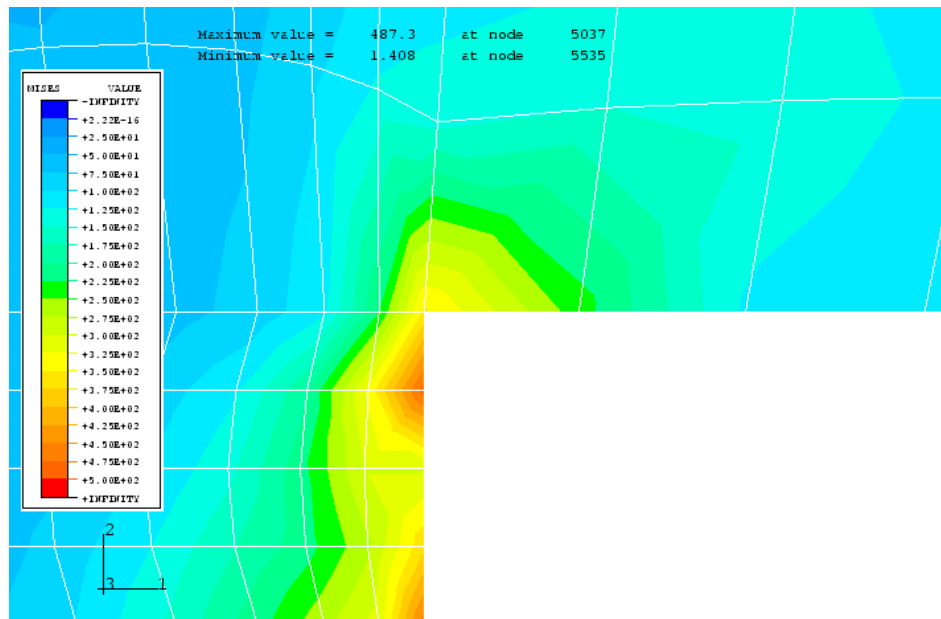


Figure 15 - Contour plot of the von Mises stresses on detail of upper clamp - zoomed view of the marked corner E (figure 14)

In the next figure 16 the surface pressure on the copper sole (line c-c' in figure 6) is plotted as a function of the x-coordinate. The surface pressure exceeds the desired value of $p=20$ MPa and the average value amounts to about $p=25.5$ MPa.

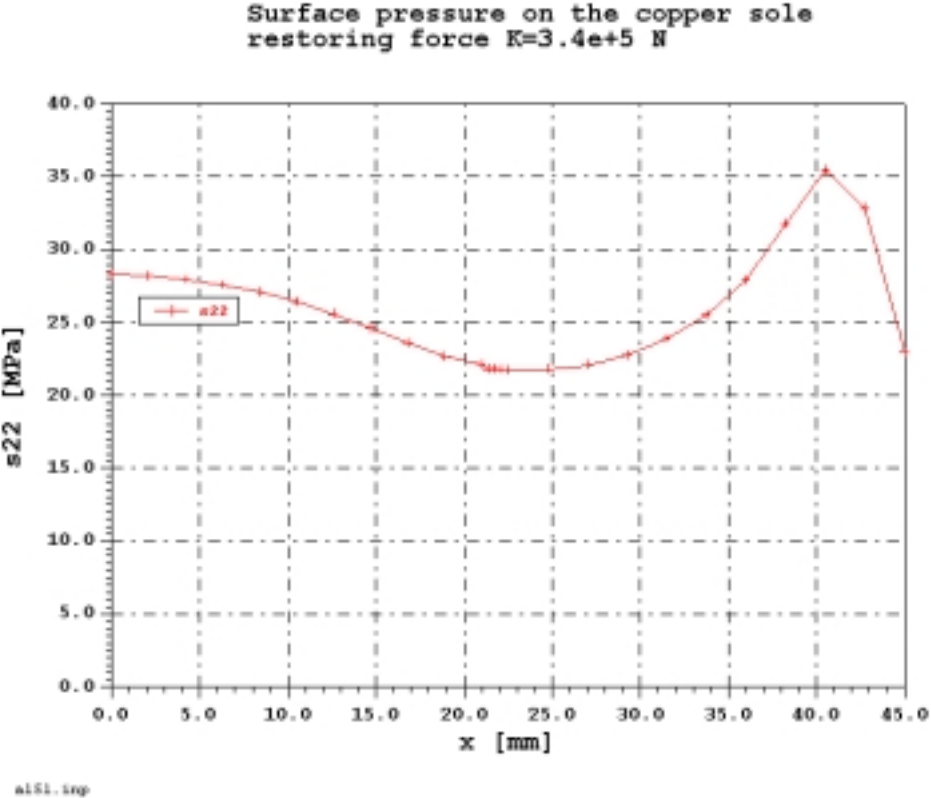


Figure 16 - Surface pressure as a function of the x-coordinate

This model was slightly modified in a second model (figure 17).

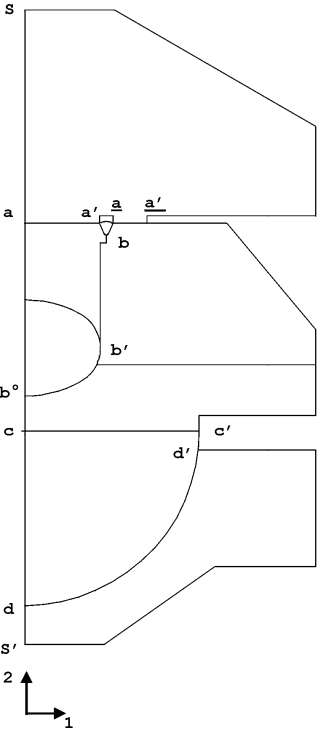
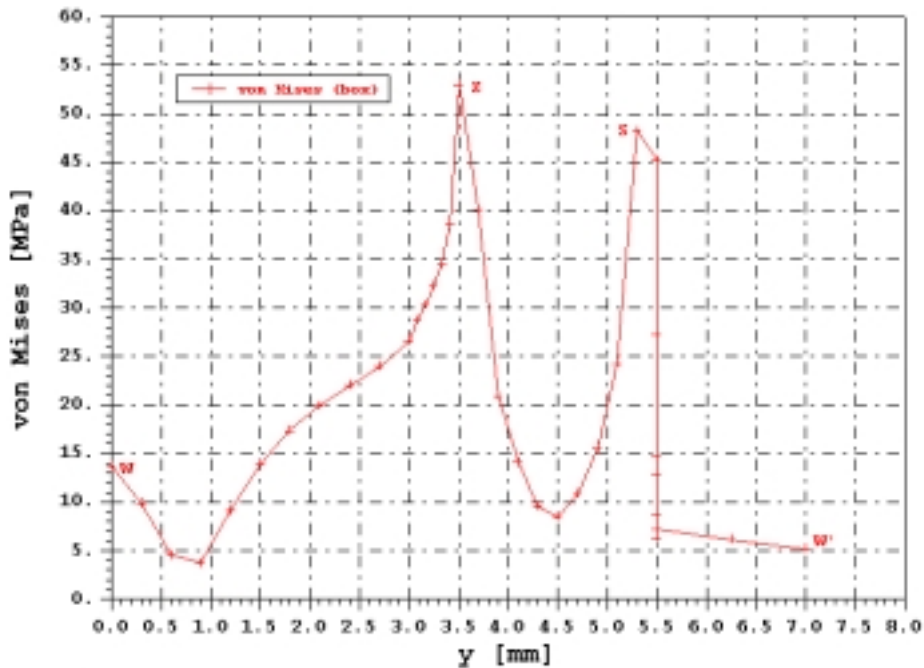


Figure 17 - Second model of the clamp joint

The contact zone was extended by 10 mm in 1-direction between the upper clamp and the box (lines a-a' and a-a').

Both small stress peaks appear again at the end of the welding seam (point Z) and at the shoulder (point S) with very small stresses below $\sigma_v=55.0$ MPa (figure 18).

'von Mises' stress along the welding seam and shoulder
restoring force $K=3.4e5$ N



a153.trp

Figure 18 - von Mises stress along the welding seam and the shoulder - 2. model marked line in figure 9

The behavior of the surface pressure on the copper sole (line c-c' in figure 6) plotted as a function of the x-coordinate in figure 19 is similar to the behavior of the first model. The pressure in the middle of the structure decreases to about 10.0 MPa and on the outer border of the copper sole increases to about $\sigma=6.0$ MPa compared with the pressure of the first model. The average value again amounts to about $p=25.5$ MPa.

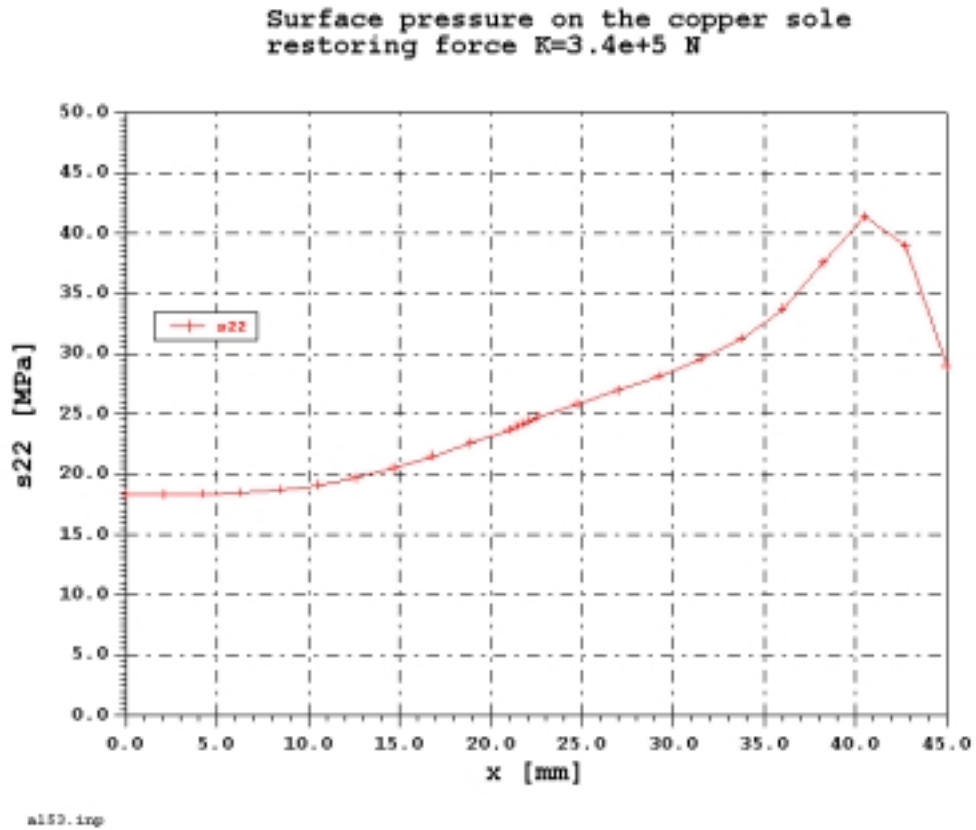


Figure 19 - Surface pressure as a function of the x-coordinate - 2. model

The average stresses of the copper parts decrease to about $\sigma_V=26.6$ MPa (part of the box) and only slightly to about $\sigma_V=23.2$ MPa (part of the lower clamp).

3. Conclusion

The calculation of the clamp joint (1st model) shows some areas with increased stress levels. The stresses are not so critical and there is no risk of structure failure. Further calculation with the 2nd model improves the stress configuration considerably.

4. References

- /1/ - ABAQUS USER MANUAL, Version 5.8,
Hibbit,Karlson & Sorensen, Inc.
- /2/ - ABAQUS/Pre Reference Guide Version 5.8
Hibbit,Karlson & Sorensen, Inc.
- /3/ - ABAQUS/Post Reference Guide Version 5.8
Hibbit,Karlson & Sorensen, Inc.